PUBLICATIONS OF THE ASTRONOMICAL SOCIETY OF THE PACIFIC
100: 1509–1521, December 1988

# COOL CIRCUMSTELLAR MATTER AROUND NEARBY MAIN-SEQUENCE STARS

H. J. WALKER

SETI Institute, 101 First Street, Los Altos, California 94022
and
NASA-Ames Research Center, Moffett Field, California 94035

AND

R. D. WOLSTENCROFT

Royal Observatory, Blackford Hill, Edinburgh, EH9 3HJ, Scotland

*Received 1988 February 8, revised 1988 August 31*

## ABSTRACT

Stars are presented which have characteristics similar to Vega and other main-sequence stars with cool dust disks, based on the *IRAS Point Source Catalog* fluxes. The objects are selected to have a 60 μm/100 μm ratio similar to Vega, β Pic, α PsA, and ϵ Eri, and they are also required to show evidence of extension in the *IRAS* Working Survey Database. The fluxes are modeled using a blackbody energy distribution. The temperatures derived range from 50 K to 650 K. The diameters of the dust disks observed by *IRAS* are estimated.

*Key words:* circumstellar matter–Vega–nearby stars–*IRAS*

## I. Introduction

Since the observation by *IRAS* of a large cool dust shell around Vega (Aumann *et al.* 1984), it has become clear that the *IRAS Point Source Catalog* must contain a significant population of these objects. Gillett (1986) reviewed the properties of the four prototype stars, Vega, β Pictoris, α Piscis Austrini, and ϵ Eridani, and presented simple models for the cool excess, based on *IRAS* survey data and on special *IRAS* slow-scan data. From the slow-scan data Gillett was able to give dust disk diameters for Vega and α PsA. The disk of β Pic has been observed optically by Smith and Terrile (1984), Gradie *et al.* (1987), and Paresce and Burrows (1987), and modeled in more detail by them, and also by Backman, Gillett, and Witteborn (1988). Using the Gliese catalog (1969) Aumann (1985) published a list of 12 candidate stars within 25 pc, including the four prototype stars in his list. Sadakane and Nishida (1986) have also prepared a list of 12 candidate stars, using criteria similar to Aumann, and they find a more normal population of binaries in their sample than occurred in Aumann's sample. Backman and Gillett (1987) have produced a list of 25 stars with excesses at 25 μm, 60 μm, or 100 μm, and color temperatures greater than 35 K, using *IRAS* coadded survey data. The new stars identified in this note are more distant than 25 pc but have characteristics very similar to those of the four prototype stars reviewed by Gillett (1986), namely Vega, β Pic, α PsA, and ϵ Eri.

## II. Selection Criteria

The candidate objects (see Table I) have been selected from the *IRAS Point Source Catalog* (version 2) using the following criteria.

1. They must be associated by the *IRAS* processing with the SAO catalog, but not with a known emission-line star.

2. They must have a 60 μm/100 μm flux density ratio (in Janskys) similar to that of the prototypes, i.e., between 0.8 and 2.0 (corresponding to a blackbody temperature range of 60 K to 150 K). Since they are associated with stars this strongly implies that the objects are detected by *IRAS* at 12 μm and 25 μm.

3. There must be evidence that the objects are extended in one or more bands. In the *IRAS* Working Survey DataBase (WSDB), which contains all the hours- or weeks-confirmed sources (see *IRAS* Explanatory Supplement 1985), the confusion status flag is set to 3 when the source is seen by three detectors in a given band. If this occurs on more than half of the focal-plane crossings, it is taken as evidence of extension in that band.

Table I is divided into three sections: prototypes, section A, and section B. Objects were relegated to section B if there was evidence that the excess seen might be due to normal mass-loss processes, such as an "e" in the spectral type denoting emission, or the presence of a companion (* given in the table), or late-type giant or supergiant. Table II contains objects which are associated with the Gliese catalog (1969). Here the objects were not required to be extended, although a few of the stars had the confusion flag set to 3 at 12 μm. Aumann's criteria were similar to ours, namely, that the sources should have been detected at 12 μm, 25 μm, and 60 μm, that they should be associated with stars in the Gliese catalog, and that they

TABLE I
OBJECTS WITH COLOR SIMILAR TO PROTOTYPE STARS

| SAO | name | sp type | R.A. | dec | 12 | 25 | 60 | 100 | V | $T_D$ | $T_{34}$ |
|---|---|---|---|---|---|---|---|---|---|---|---|
| | | | 1950 | | [12] | [25] | [60] | [100] | (B-V) | $T_*$ | $E_{B-V}$ |
| PROTOTYPES | | | | | | | | | | | |
| 234134 | β Pic | A5V | 05 46 05.4 | −51 04 55 | 4.07* | 9.38* | 18.86* | 10.79* | 3.84 | 105 | 125 |
| | | | | | 2.1 | −0.4 | −3.0 | −3.5 | 0.17 | 10000 | 0.0 |
| 67174 | Vega | A0V | 18 35 15.0 | +38 44 16 | 29.79 | 9.36* | 9.01* | 7.54* | 0.04 | 95 | 85 |
| | | | | | −0.1 | −0.4 | −2.2 | −3.1 | 0.00 | 12000 | 0.0 |
| 191524 | α PsA | A3V | 22 54 54.5 | −29 53 23 | 13.20 | 4.27 | 9.11* | 11.19* | 1.16 | 80 | 60 |
| | | | | | 0.8 | 0.5 | −2.2 | −3.5 | 0.09 | 12000 | 0.0 |
| 130564 | ε Eri | K2V+ | 03 30 32.2 | −09 37 34 | 6.90 | 2.21 | 1.59 | 1.87 | 3.73 | 90 | 65 |
| | | | | | 1.5 | 1.2 | −0.3 | −1.6 | 0.88 | 5000 | 0.0 |
| SECTION A | | | | | | | | | | | |
| 147886 | 49 Cet | A3V | 01 32 11.8 | −15 55 55 | 0.42 | 0.42 | 2.05* | 1.87* | 5.63 | 80 | 75 |
| | | | | | 4.6 | 3.0 | −0.6 | −1.6 | 0.1 | 12000 | 0.0 |
| 112630 | HD34700 | G0 | 05 17 00.6 | +05 35 41 | 0.71 | 4.97 | 13.85* | 9.02* | 8.8 | 100 | 105 |
| | | | | | 4.0 | 0.3 | −2.7 | −3.3 | 1.2 | 6000 | 0.6 |
| 77144 | HD35187 | A2 | 05 20 56.7 | +24 54 55 | 6.27 | 10.95* | 7.29* | 4.82* | 8.2 | 170 | 105 |
| | | | | | 1.6 | −0.5 | −2.0 | −2.6 | 0.1 | 12000 | 0.0 |
| 26804 | HD233517 | A2 | 08 18 59.8 | +53 14 27 | 0.53 | 3.96* | 7.38* | 4.81* | 9.4 | 105 | 105 |
| | | | | | 4.3 | 0.6 | −2.0 | −2.6 | 1.4 | 5000 | 0.5 |
| 206462 | HD135344 | A0V | 15 12 37.5 | −36 58 15 | 1.92 | 7.29 | 26.27* | 25.44* | 8.7 | 85 | 70 |
| | | | | | 2.9 | −0.1 | −3.4 | −4.4 | 0.6 | 13500 | 0.6 |
| 226057 | HD139614 | A7V | 15 37 22.5 | −42 20 14 | 4.95 | 18.61 | 18.29* | 13.53 | 8.2 | 135 | 90 |
| | | | | | 1.9 | −1.1 | −3.0 | −3.8 | 0.1 | 12000 | 0.0 |
| 183956 | HD142666 | A3 | 15 53 42.9 | −21 53 00 | 9.32* | 10.33* | 6.73 | 5.30* | 8.8 | 175 | 95 |
| | | | | | 1.2 | −0.5 | −1.9 | −2.7 | 0.4 | 12000 | 0.3 |
| 184124 | HD144432 | A9/F0V | 16 03 53.6 | −27 35 08 | 8.19 | 8.63* | 5.19* | 3.15 | 8.0 | 180 | 115 |
| | | | | | 1.4 | −0.3 | −1.6 | −2.2 | 0.5 | 8500 | 0.2 |
| 186777 | HD169142 | B9V | 18 21 18.0 | −29 48 30 | 3.51 | 19.82 | 28.85* | 22.74* | 8.1 | 115 | 85 |
| | | | | | 2.3 | −1.2 | −3.5 | −4.3 | 0.1 | 18000 | 0.2 |
| SECTION B | | | | | | | | | | | |
| 179815 | HD98800 | K5V* | 11 19 35.6 | −24 30 02 | 2.39 | 9.28 | 6.68 | 4.29* | 9.5 | 165 | 110 |
| | | | | | 2.7 | −0.4 | −1.9 | −2.5 | 1.1 | 4500 | 0.0 |
| 239288 | HD101584 | MIII* | 11 38 33.9 | −55 17 49 | 102.9 | 134.9 | 178.7 | 99.05* | 7.0 | 120 | 130 |
| | | | | | −1.4 | −3.3 | −5.4 | −5.9 | 0.4 | 7500 | 0.0 |
| 256895 | HD104237 | A0pe | 11 57 32.7 | −77 54 47 | 24.51 | 23.91 | 13.51 | 9.21* | 6.5 | 190 | 100 |
| | | | | | 0.2 | −1.4 | −2.6 | −3.3 | 0.2 | 14500 | 0.2 |
| 240664 | HD114855 | F5Iab | 13 11 05.0 | −54 25 43 | <0.31 | 2.54 | 7.53* | 5.18 | 8.3 | 95 | 100 |
| | | | | | >4.9 | 1.1 | −2.0 | −2.7 | 0.9 | 7500 | 0.4 |
| 140789 | HD141569 | A0Ve | 15 47 20.1 | −03 46 13 | 0.66 | 1.99 | 5.37* | 3.34 | 7.1 | 95 | 110 |
| | | | | | 4.1 | 1.3 | −1.6 | −2.2 | −0.1 | 17000 | 0.0 |
| 226389 | HD142527 | F6III | 15 53 16.8 | −42 10 46 | 12.07 | 22.23 | 106.2 | 82.23* | 8.2 | 80 | 85 |
| | | | | | 0.9 | −1.3 | −4.9 | −5.7 | 0.8 | 7000 | 0.3 |
| 183986 | HD143006 | G5e | 15 55 38.9 | −22 48 45 | 1.04 | 3.36 | 6.44 | 4.68* | 10.3 | 105 | 95 |
| | | | | | 3.6 | 0.8 | −1.8 | −2.6 | 1.0 | 5500 | 0.3 |
| 257579 | BR Oct | M5 | 18 12 34.8 | −77 41 30 | 39.40* | 17.50* | 2.88* | 1.85 | 8.8 | 600 | 105 |
| | | | | | −0.4 | −1.0 | −1.0 | −1.6 | 1.7 | 3000 | 0.0 |
| 87856 | HD188037 | A2* | 19 50 20.8 | +22 19 28 | 203.3 | 84.70 | 11.02* | 12.39* | 8.0 | 650 | 65 |
| | | | | | −2.1 | −2.8 | −2.4 | −3.7 | 0.9 | 12000 | 0.8 |

Notes to table I
All fluxes and magnitudes are color-corrected
V comes from either the Bright Star Catalogue or the Strasbourg Bibliography
* in the spectral type column denotes double star
* in the flux column denotes extension detected in that band

Notes to Table I (Continued)

SAO 130564: suspected astrometric binary by van de Kamp (1971)
SAO 183956: SAO catalogue gives $m_V = 8.2$
SAO 179815: noted in Heintz (1980) list of double stars. SAO catalogue gives $m_V = 8.6$.
SAO 239288: noted in new Bright Star Catalogue as having a shell, the original spectral type was F2, later classification F0Iape. Humphreys (1976) finds it to be binary, M giant with a late B/early A giant companion.
SAO 140789: Gahm et al. (1983) note it as binary, with A0V (V=7.1) and G0Vpec (V=12.7), their spectral type and V for the primary alone are used here.
SAO 226389: noted by Odenwald (1986) of possibly being a T Tau star.
SAO 183986: noted by Odenwald (1986) as possibly being a T Tau star. Stephenson (1986) notes it in his list as having H$\alpha$ emission. SAO catalogue gives $m_V = 10.3$.
SAO 87856: Lee (1970) include it in a list high luminosity M stars, so this is probably the other component of the binary, and hence will influence the IRAS fluxes.

TABLE II
OBJECTS WITH GLIESE ASSOCIATION

| SAO | name | sp type | R.A. | dec | 12 | 25 | 60 | 100 | V | $T_D$ | |
|---|---|---|---|---|---|---|---|---|---|---|---|
| | | | 1950 | | [12] | [25] | [60] | | (B-V) | $T_*$ | $E_{B-V}$ |
| 21133 | $\beta$ Cas | F2IV | 00 06 32.2 | +58 52 19 | 8.24* | 2.25 | 0.83 | <12.66 | 2.27 | 150 | |
| | | | | | 1.3 | 1.2 | 0.4 | | 0.34 | 8000 | |
| 22268 | $\delta$ Cas | A5III-IV | 01 22 32.1 | +59 58 25 | 3.42* | 0.87 | 0.28: | <6.09 | 2.60 | 170 | |
| | | | | | 2.3 | 2.2 | 1.6: | | 0.13 | 11000 | |
| 168373 | $\alpha$ For | F8IV* | 03 09 57.7 | −29 10 37 | 2.85* | 0.74 | 0.23: | <1.00 | 3.85 | 170 | |
| | | | | | 2.5 | 2.4 | 1.8: | | 0.51 | 7000 | |
| 233457 | $\gamma$ Dor | F4III | 04 14 43.3 | −51 36 37 | 1.20 | 0.37 | 0.28: | <1.00 | 4.24 | 95 | |
| | | | | | 3.4 | 3.2 | 1.6: | | 0.31 | 8000 | |
| 5496 | HD33564 | F6V | 05 14 15.5 | +79 10 44 | 0.79 | 0.21: | 0.26: | <1.00 | 5.04 | 65 | |
| | | | | | 3.9 | 3.8: | 1.7: | | 0.47 | 7000 | |
| 236232 | $\delta$ Vel | A1V* | 08 43 19.9 | −54 31 31 | 5.76* | 1.52 | 0.42 | <8.76 | 1.95 | 250 | |
| | | | | | 1.7 | 1.6 | 1.1 | | 0.04 | 14000 | |
| 99809 | $\beta$ Leo | A3V* | 11 46 28.9 | +14 51 06 | 5.26 | 1.75 | 1.02 | <1.00 | 2.14 | 140 | |
| | | | | | 1.8 | 1.5 | 0.2 | | 0.08 | 12500 | |
| 241315 | HD121384 | G6IV-V | 13 53 14.1 | −54 27 33 | 0.72 | 0.17: | 0.37: | <10.23 | 6.0 | 50 | |
| | | | | | 4.0 | 4.0: | 1.3: | | 0.78 | 5500 | |
| 226064 | HD139664 | F5IV-V | 15 37 44.7 | −44 29 57 | 1.24 | 0.62 | 0.59 | <2.37 | 4.64 | 120 | |
| | | | | | 3.4 | 2.6 | 0.8 | | 0.40 | 7500 | |
| 208591 | HD155826 | F7V+G2V | 17 12 09.4 | −38 32 22 | 4.12 | 5.30 | 8.14 | <260.2 | 5.96 | 115 | |
| | | | | | 2.1 | 0.3 | −2.1 | | 0.58 | 6500 | |
| 230846 | HD207129 | G0V | 21 45 01.5 | −47 32 07 | 0.59 | 0.19: | 0.23: | <1.00 | 5.59 | 60 | |
| | | | | | 4.2 | 3.9: | 1.8: | | 0.60 | 6000 | |
| 35498 | HD221354 | K2V | 23 28 57.8 | +58 52 52 | 0.41 | 0.18: | 0.90: | <20.51 | 6.7 | 70 | |
| | | | | | 4.6 | 3.9: | 0.3: | | 0.83 | 5500 | |

Notes to table II
All fluxes and magnitudes are color corrected
V comes from either the Bright Star Catalogue or the Strasbourg Bibliography
* in the spectral type column denotes double star
* in the flux column denotes extension detected in that band
SAO168373: The secondary is G7V (Edwards, 1976)
SAO99809: This is a short period $\delta$ Scuti star according to Halprin and Moon (1983).

should have a significant excess at 60 $\mu$m. He included in his list *IRAS* sources which associated with high proper-motion Gliese stars; these were not correctly associated in the original *IRAS* catalog so were not included in our list. Aumann's preliminary list (his Table I) contains all of our objects in Table II. 49 Ceti, in Table I, is also in Sadakane and Nishida's list.

All the fluxes and magnitudes shown in Tables I and II are color corrected. An asterisk in the flux column of Table I and Table II indicates that the source is extended in that band. A point source crossing the focal plane of *IRAS* will normally trigger two detectors in any given band. It is, however, possible for the point source to pass across the edge of adjacent detectors and the middle of a third detector (on the other side of the focal plane) in which case the confusion status flag is set to 3 in the WSDB (see Explanatory Supplement for further information on CSTAT). If the source is slightly extended there will be more opportunities for it to trigger three detectors. Thus, if three detectors are triggered on more than half the crossings this is good evidence that the source is slightly extended: This corresponds to a minimum of three out of four crossings. For confusion with cirrus, the confusion flag is set to a number higher than 3. An upper limit to the diameter of the source is set by the fact that the source is in the *Point Source Catalog* rather than the *Small Scale Structure Catalog*, so it has a diameter of less than 2 arc min (12 μm, 25 μm), 4 arc min (60 μm), and 8 arc min (100 μm). Aumann *et al.* (1984) showed that Vega was not extended at 12 μm and was extended at 60 μm, relative to the genuine point sources β Gruis and α Bootis. Table I shows that Vega is not flagged as extended at 12 μm and is at 60 μm. Special measurements at 60 μm of Vega and α PsA using *IRAS* slow scans (as part of the pointed observation program) yielded diameters of 25 × 29 arc sec and 36 × <13 arc sec, respectively, after deconvolution (Gillett 1986): Both these objects were flagged with confusion status 3 at 60 μm in the WSDB verifying that this flag is sensitive to slight extensions.

## III. Discussion

The *IRAS* colors of the sources are displayed in Figures 1(a) and 1(b). The magnitudes (given in Tables I and II) are derived from the color-corrected fluxes. Figure 1 shows the blackbody line and three boxes, which are the zones of normal (non-color-corrected) colors for bright stars (1), carbon-rich stars (2), and oxygen-rich stars (3), from Walker and Cohen (1988). In Figure 1(b) the zone for bright stars and oxygen-rich stars is identical. Our 60 μm/100 μm ratio translates to a range in [60] − [100] color of 0.4 to 1.4, and most of the objects fall within a [25] − [60] color range of 1 to 4. The two exceptions are BR Octantis, an M 5 star, and SAO 87856, a double star, both belonging to section B of Table I; they have [25] − [60] < 0.0. These two stars are well separated from the rest in the [12] − [25] versus [25] − [60] diagram and are found in the zone showing normal colors for oxygen-rich stars with circumstellar dust. The objects with Gliese association (Table II) lie closer to the normal colors than those in Table I, but both groups lie clear of the blackbody line. This reflects the fact that, like Vega, α PsA, and ε Eri, the Gliese objects have very little excess at 12 μm and 25 μm so that their [12] − [25] color is close to the value expected for a normal stellar photosphere (i.e., 0.0). There are two exceptions (with [12] − [25] > 0.5),

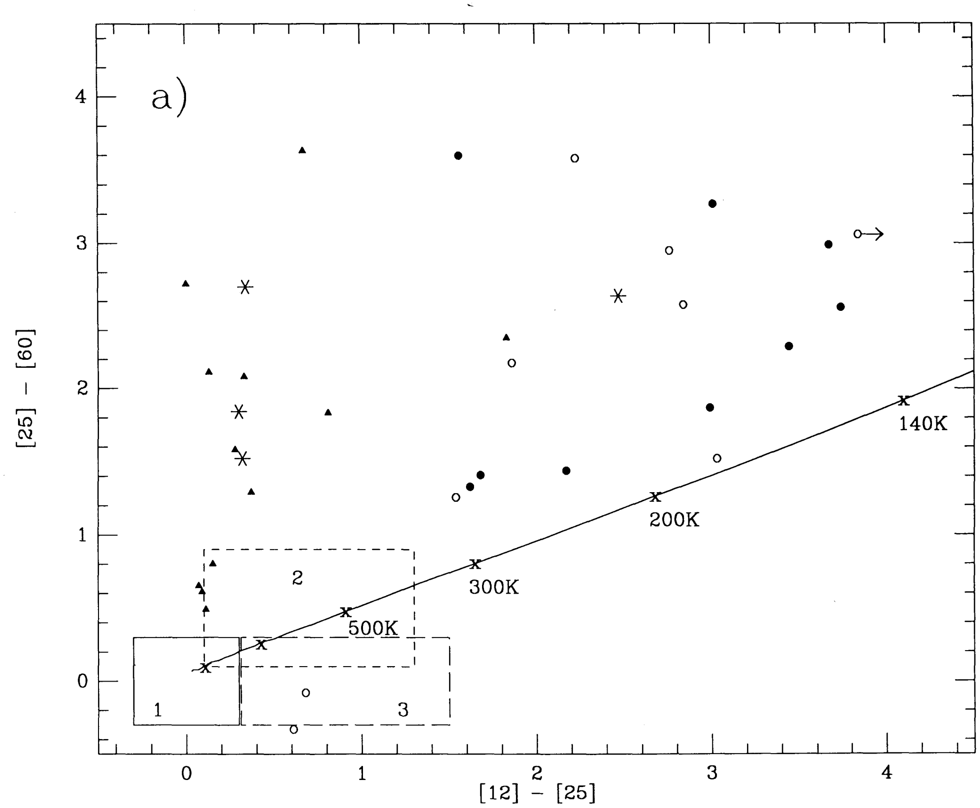


FIG. 1a–The *IRAS* color-color diagrams showing the prototypes (*), Table I section A (•), Table I section B (○), Table II (▲), with zones for normal stars from Walker and Cohen (1988), the bright stars (1), C-rich stars (2), O-rich stars (3), and a blackbody line. The last two points on the blackbody line are 1000 K and 5000 K.

SAO 226064 (HD 139664) and a binary SAO 208591 (HD 155826). The objects in Table I are similar to β Pic in that most of their 12 μm flux comes from the cool dust and not from the star. In the [25] − [60] versus [60] − [100] diagram most of the objects lie close to the blackbody line, showing they are surrounded by cool dust with almost a blackbody energy distribution. β Pic is a noticeable exception to the Gliese catalog stars in that its 12 μm flux is dominated by the cool dust. Figure 1 of Gillett (1986) illustrates this very clearly, since the other prototype stars all have upper limits for the 12 μm excess flux. However, a recent model of β Pic by Backman *et al.* (1988) for the *IRAS* and near-infrared data required a dust-free zone of radius 15 to 20 AU, which reflects a deficit of observed flux at 12 μm. Three objects with the highest [12] − [25] color are SAO 112630, SAO 26804, and SAO 186777. Although the luminosity class of the first two stars is unknown, the spectral classes of G0 and K2 are such that the *IRAS* colors clearly indicate the presence of circumstellar dust. SAO 186777 (B9 V) appears to be a normal main-sequence star which is not losing mass.

*B* and *V* were used to fit a stellar photosphere (blackbody), after dereddening, giving $T_*$ in Table I. $(B-V)$ was used even when the resulting temperature disagreed with that expected from the spectral type and luminosity class ($T'_*$ in Table III): This approach was taken to allow us to assemble a more uniform set of data, since a number of stars had no luminosity class. After subtracting the model stellar flux, the excess fluxes in the *IRAS* domain were fitted by a cool blackbody (see Fig. 2) to give $T_D$ in Tables I and II. The 25 μm and 60 μm fluxes were used to determine the fit of the cool blackbody curve, and in many cases (including β Pic) the 12 μm point was conspicuously above the model fit. This shows that a more detailed model is needed, with grain size distribution (see, for example, Backman *et al.* 1988), but with only three or four data points that would be inappropriate here. If data were available at other wavelengths for these stars a more detailed model would be suitable. For Vega the stellar model was not placed precisely through *B* and *V* since the 12 μm point was also considered in the model fit. The scales for the model fluxes were fixed using the *V* and 60 μm points, except for the dust model of SAO 257579, where the 12 μm point was used, and SAO 87856, where the 25 μm point was selected. Figure 2 shows very clearly that for most of the stars in Table I the *IRAS* fluxes are not influenced by the flux from the stellar photosphere. The Gliese catalog stars (Table II) have much smaller flux excesses in the *IRAS* wavebands, and Figure 2 shows that

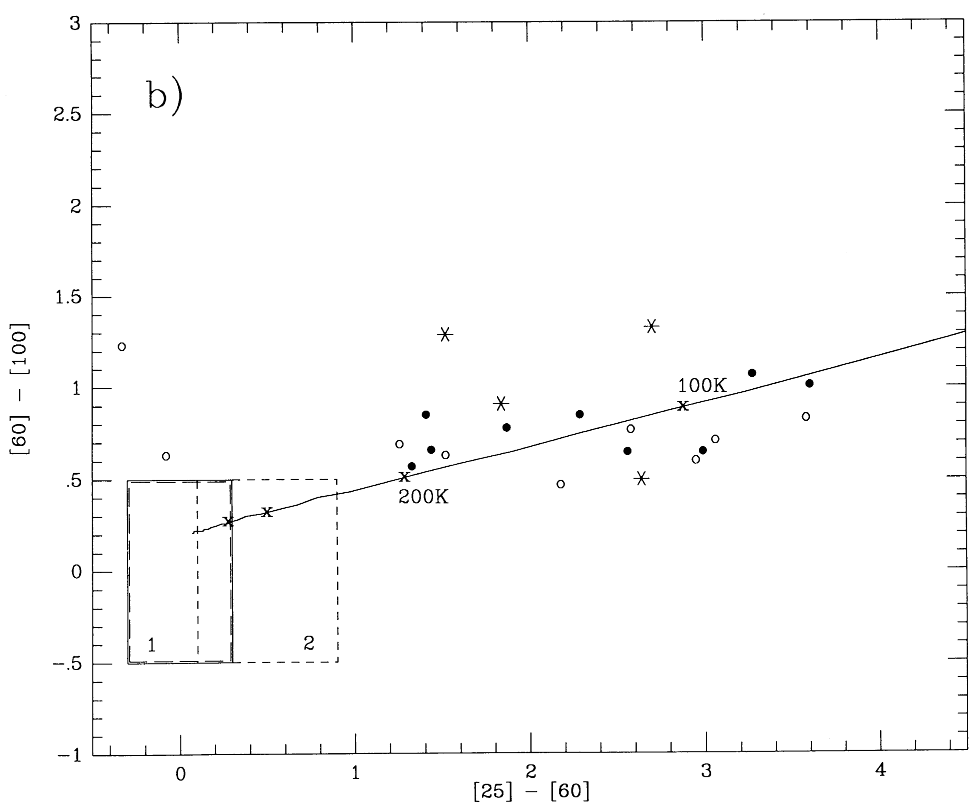


FIG. 1b–The *IRAS* color-color diagrams showing the prototypes (*), Table I section A (•), Table I section B (○), Table II (▲), with zones for normal stars from Walker and Cohen (1988), the bright stars (1), C-rich stars (2), O-rich stars (3), and a blackbody line. The last two points on the blackbody line are 500 K and 1000 K.

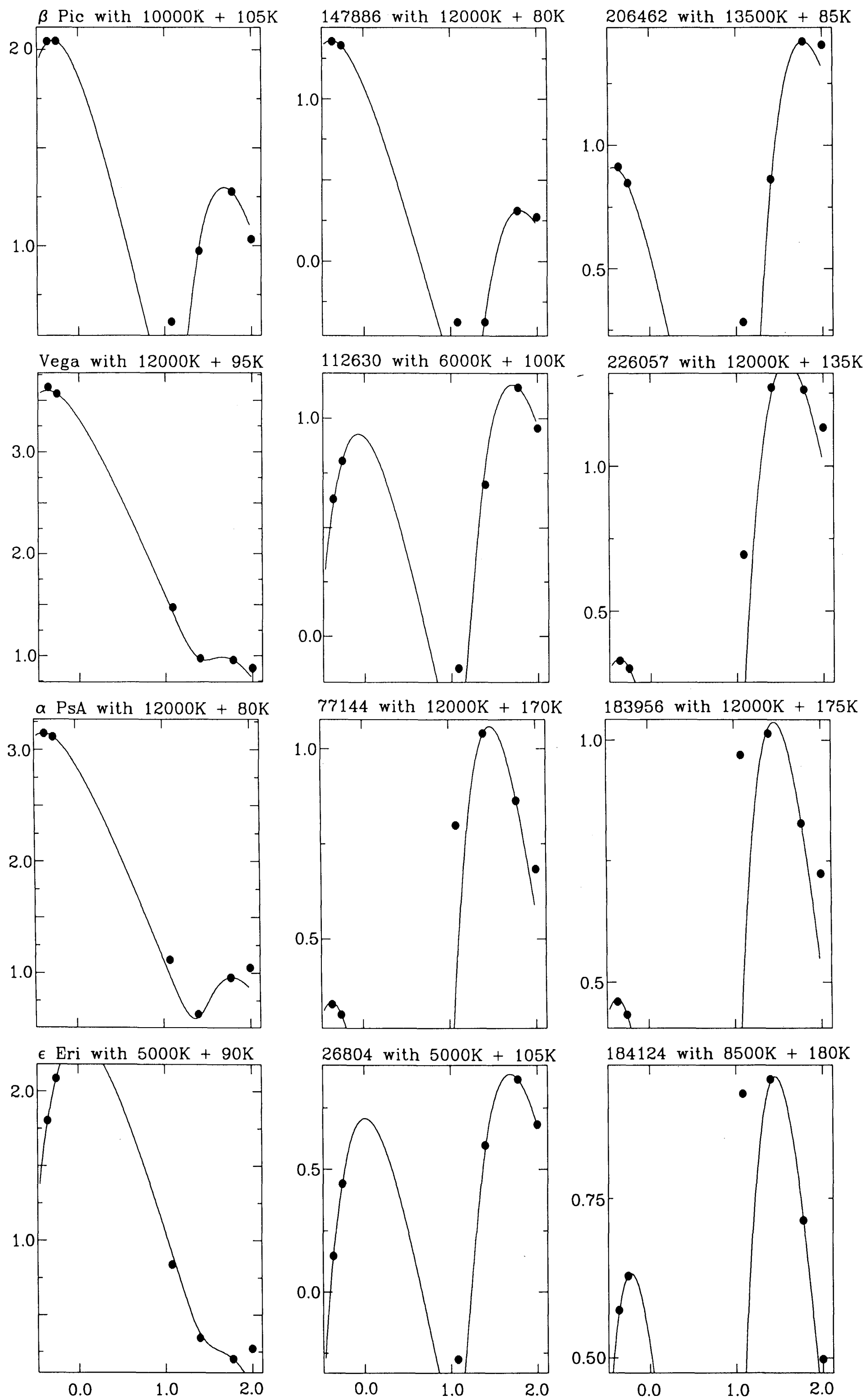


FIG. 2a–Energy distributions and blackbody fits for the stars in Table I. Log (flux density in Janskys) is plotted against log (wavelength in microns).

for all these stars, except SAO 208591, the *IRAS* 12 μm flux is dominated by the stellar photosphere and not the dust excess. Here the 25-μm flux is also influenced by the stellar photosphere. For stars above 8000 K the error in estimating the temperature using $B$ and $V$ is large (compared with the value derived from the spectral type, $T'_*$ in

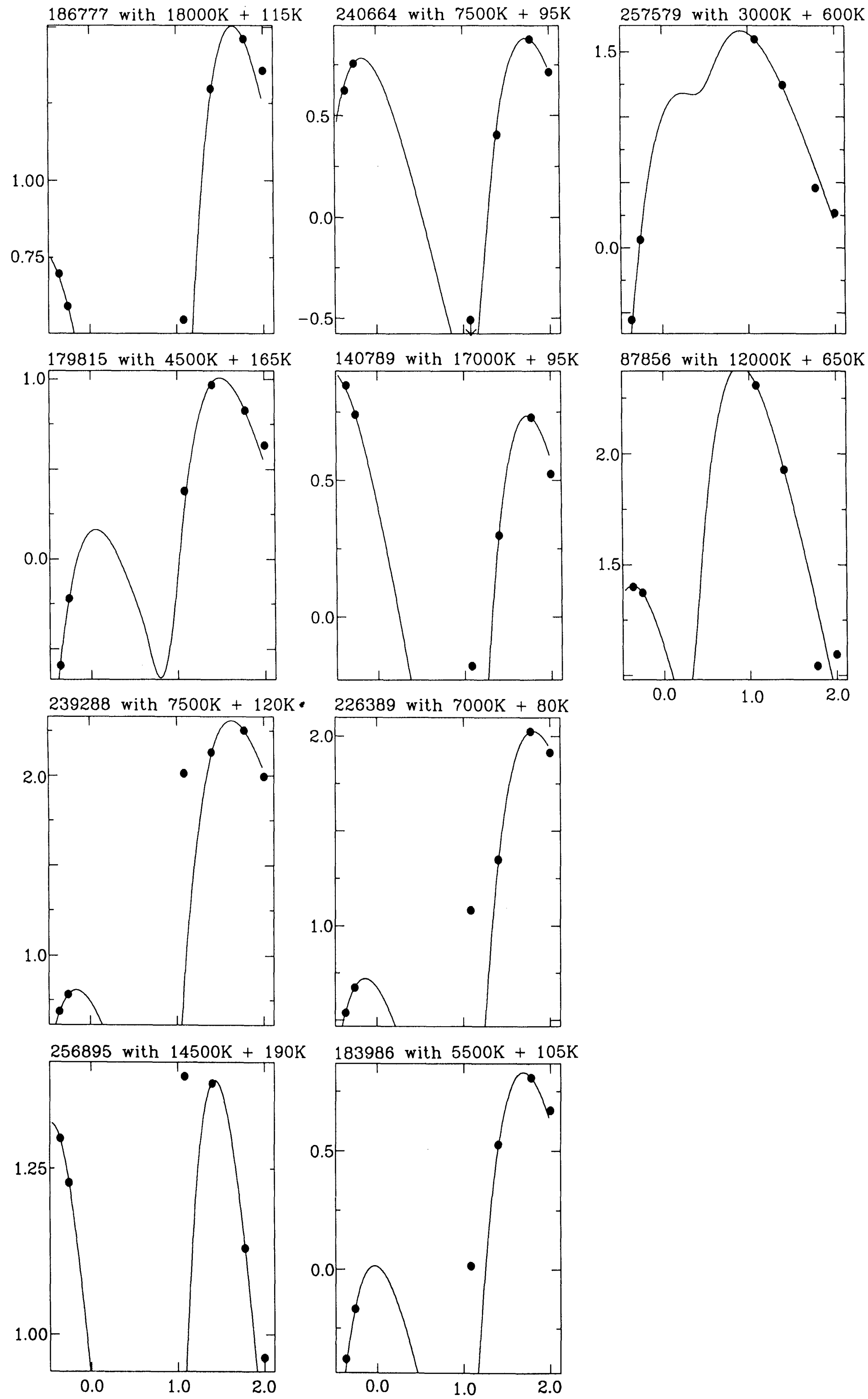


FIG. 2b–Energy distributions and blackbody fits for the stars in Table I. Log (flux density in Janskys) is plotted against log (wavelength in microns).

Table III); however, the contribution to the *IRAS* wavebands is relatively insensitive to the temperature since it is on the tail of the Rayleigh-Jeans energy distribution. Consequently, a large change in stellar temperature makes only a small change in 12 μm flux.

Our selection criterion results in a very narrow distribution of $T_{34}$ (see Fig. 3(a)). The distribution of $T_D$ is broader and asymmetric, with a peak between 90 K and

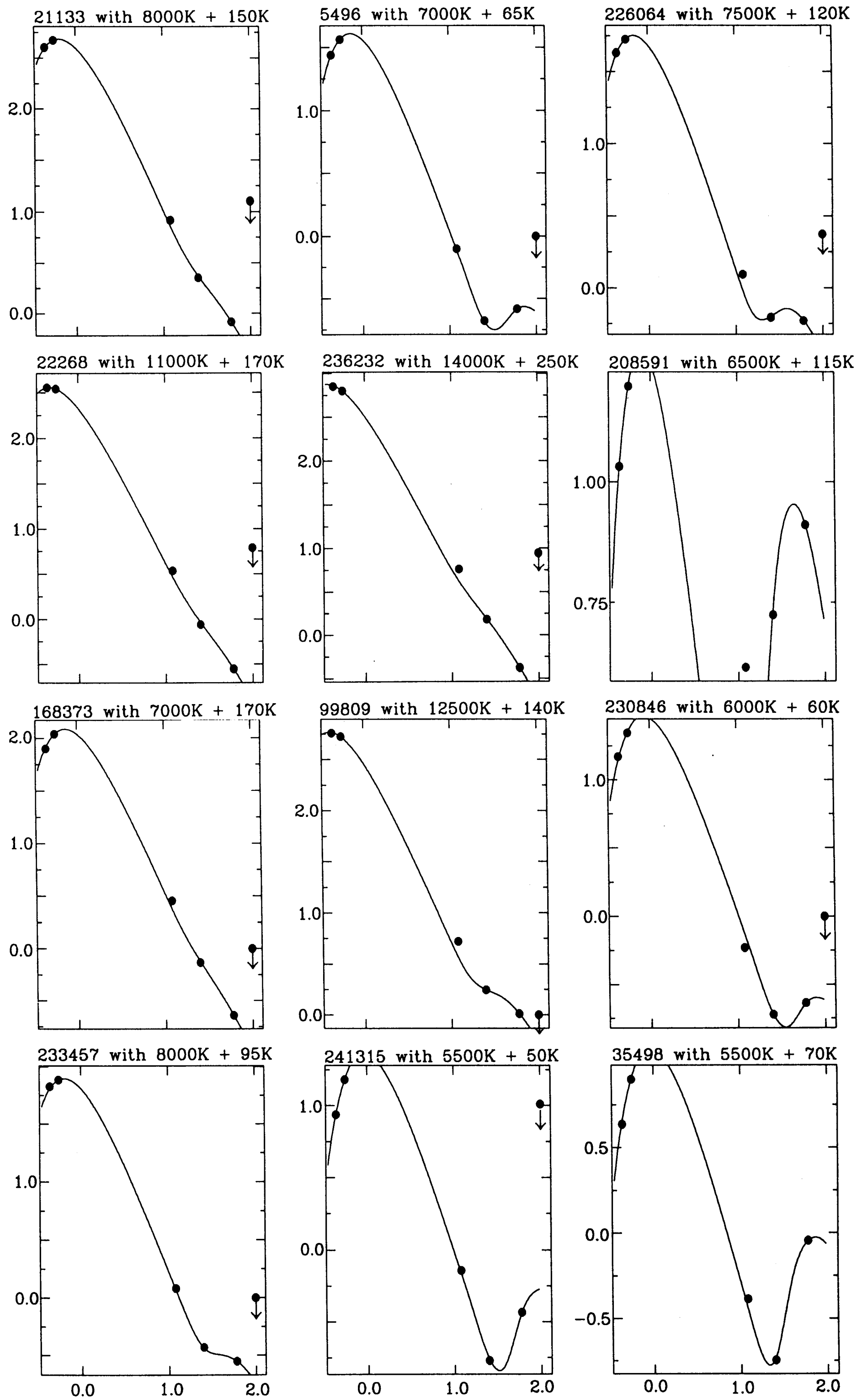


FIG. 2c–Energy distributions and blackbody fits for the stars in Table I. Log (flux density in Janskys) is plotted against log (wavelength in microns).

120 K, and a tail toward higher temperature (see Fig. 3(b)). The last bin in Figure 3(b) contains all the sources with $T_D > 210$ K. The sharp cutoff at $T_D = 60$ K is due to our selection criterion in the total flux ratio, viz. $F_{60}/F_{100} \geq 0.8$. The upper limit set in the total flux ($F_{60}/F_{100} \leq 2.0$) introduces a higher temperature limit which is significantly influenced by the stellar contribution (cf. BR Oct). If selection effects could be discounted in the tempera-

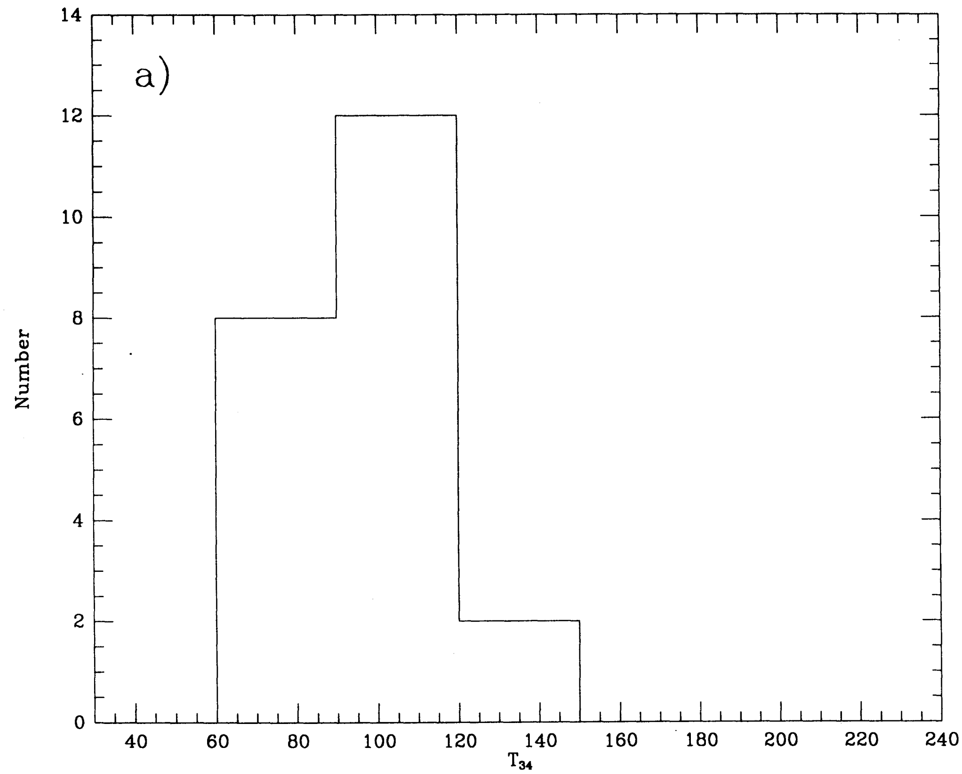


FIG. 3a–The distribution of dust shell temperatures from the flux ratio 60 μm/100 μm.

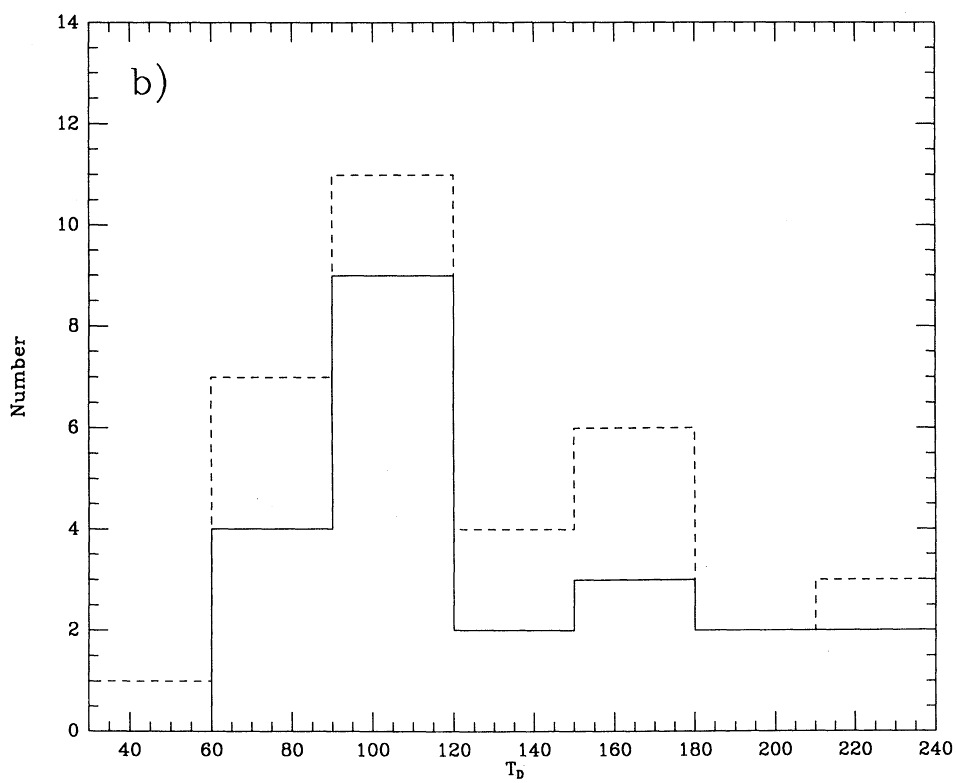


FIG. 3b–The distribution of dust shell temperatures from the model fit. The dashed line includes the stars in Table II (which do not have 100 μm fluxes).

ture range 90 K to 210 K, the $T_D$ histogram would contain information on the size distribution of the disks: However, we suspect that selection effects do in fact dominate.

Detailed models of the four prototype stars (Gillett 1986; Backman *et al.* 1988) indicate that the shells are extensive with outer radii in the range 250 AU to 790 AU. The temperature varies throughout the shell, for example between 45 K and 210 K in the case of β Pic. This modeling is possible when either *IRAS* slow scans or ground-based multiaperture infrared photometry is available in addition to the *IRAS* fluxes. This information is not available for the stars in sections A and B of Table I and in Table II; therefore, we adopt the approach suggested by Aumann (1985) in order to assess a characteristic size of the dust shells. This involves fitting a single blackbody to the excess *IRAS* flux to determine first a disk temperature, as described above, and then an effective disk radius, $R_D$, based on the following energy balance equation for a grain of radius "a" at a distance $R_D$ from the star (*).

$$\frac{\pi a^2}{4\pi R_D^2} 4\pi R_*^2 \sigma T_*^4 \langle\epsilon_{vis}\rangle = 4\pi a^2 \sigma T_D^4 \langle\epsilon_{IR}\rangle$$

where $\epsilon$ is the emissivity. This gives

$$\frac{R_D}{R_*} = 0.5 \left(\frac{T_*}{T_D}\right)^2 \left\langle\frac{\epsilon_{vis}}{\epsilon_{IR}}\right\rangle^{1/2} .$$

In order to compare disks we assume that the emissivity factor is unity. In Table III we show the radii $R_D$ and $R_{34}$ corresponding to the derived temperatures $T_D$ and $T_{34}$. The stellar temperature ($T_*'$) was taken from Allen's (1973) compilation of effective temperatures for various spectral types and luminosity classes. In this table we also show distances derived either from trigonometric parallax measurements or using absolute magnitudes derived from spectral classification (values taken from Allen 1973) with no reddening correction. In Figure 4 the relation between effective disk radius and the star distance (from the Earth) is shown for the two derived temperatures. The radii derived from $T_{34}$ are larger than those associated with $T_D$ showing that they represent dust in the cooler parts of the disk. For the two prototypes clearly resolved in the *IRAS* slow-scan experiments, the angular diameters deduced in our analysis, about 10 arc sec for both Vega and α PsA, agree well with the slow-scan diameters of 25 × 29 arc sec (Vega) and 36 × < 13 arc sec (α PsA) (Gillett 1986). The fact that ϵ Eri and β Pic were not resolved is consistent with our diameters. For the objects in sections A and B of Table I there is a trend of increasing disk size with distance, with a clear absence of small disks at large distances. The nominal angular sizes lie between 0.1 and 1.0 arc sec (with the exception of 49 Cet): These are clearly too small to trigger a confusion flag, so we conclude that a single temperature assumption is producing an underestimate of $R_D$. Despite the nonresolution of

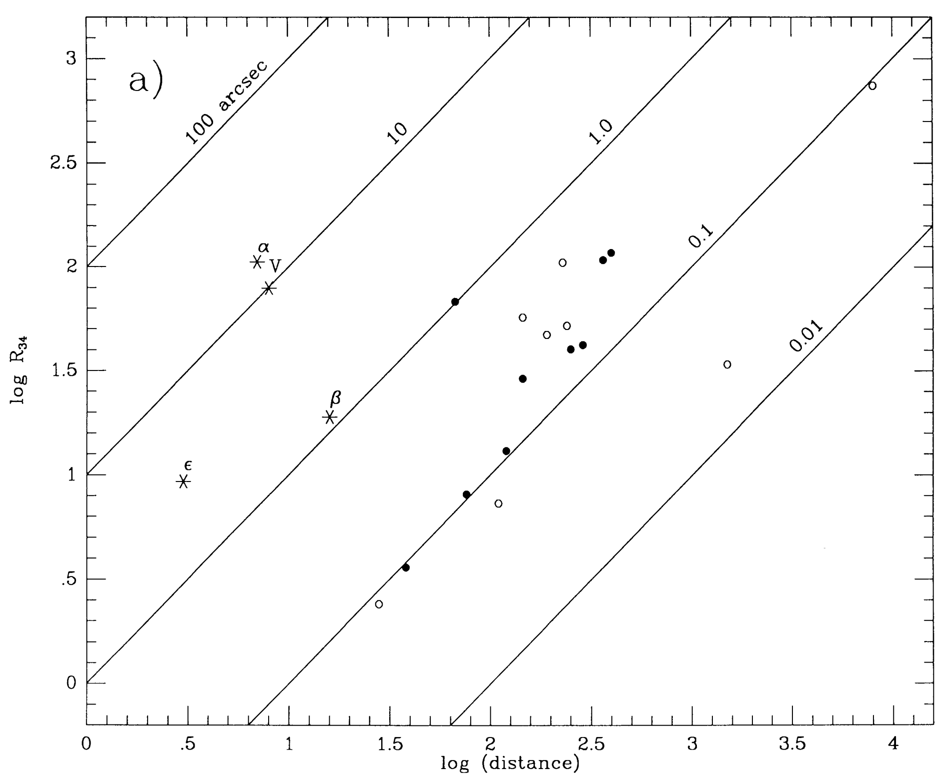


FIG. 4a–The distance to the star in parsecs is plotted against the radius of the dust shell in AU for the prototypes (*), Table I section A (●), Table I section B (○), Table II (▲), flux ratio data. The prototype stars are labeled.

β Pic with the *IRAS* slow scans, it is known from coronographic imaging by several groups (Smith and Terrile 1984; Gradie *et al.* 1987; Paresce and Burrows 1987) that the major axis diameter is 75 arc sec: This discrepancy is attributed to a nonfavorable *IRAS* scan orientation and perhaps also to the presence of small grains. In Figure 4(b) the disk radii associated with $T_D$ (which depends most strongly on the 25 μm to 60 μm ratio for the excess flux) are smaller, as indicated earlier. The objects from the Gliese catalog (Table II) are included and tend to show somewhat larger angular diameters than those from sections A and B. In both figures 49 Cet is conspicuous in terms of its large angular size, comparable to that of β Pic. In Figure 4(b) the star from the Gliese catalog close to β Pic is SAO 233457 (γ Doradus), and the other four stars close to the 1 arc sec line are SAO 5496 (HD 33564), SAO 99809 (β Leo), SAO 241315 (HD 121384), and SAO 230846 (HD 207129). The two stars with very small angular diameters in Figure 4(b) are SAO 87856 (HD 188037) and SAO 179815 (HD 98800).

If the *IRAS* excess emission was caused by normal mass-loss processes, due either to a young star or an evolved star losing mass, CO would be observed. The 5 m Millimeter Wave Observatory telescope (in Texas) was used to observe the CO $J = 1$–$0$ transition (115 GHz, 2.6 mm) at the positions of the stars in Tables I and II, and also for the objects in Aumann's Table I not on our lists, with a detection limit of around $10^{16}$ molecules/cm$^2$. For four sources CO was detected along the line of sight, noted in Table III by "Y", all at low galactic latitudes: Those stars observed, but with no CO detected, are marked with "N" in Table III. For none of the stars with CO detected did the CO have the same radial velocity as the star, so it is assumed that the CO is not associated with the star, and it is likely that the anomalous *IRAS* fluxes are also a chance alignment. If this is so, the "cloud" in the line of sight is of very small angular size.

## IV. Conclusions

As noted before by Aumann (1985) the A stars dominate the samples, but this is a selection effect arising from the *IRAS* sensitivity and the efficiency of A-star dust heating. The sample of fainter stars from Backman and Gillett (1987) shows that this is not a real effect, since their spectral types are more uniformly distributed. The stars presented here have similar *IRAS* characteristics to the prototype objects, but more data are needed so that detailed modeling can be done. It is unlikely that these disks can be detected by imaging, in the manner of β Pic, since they have smaller angular size, so the confirmation of their nature must be less direct. The lack of CO is one indication that these are not normal circumstellar dust shells associated with mass-loss processes.

The *Infrared Astronomical Satellite* (*IRAS*) was developed and operated by the U.S. National Aeronautics and

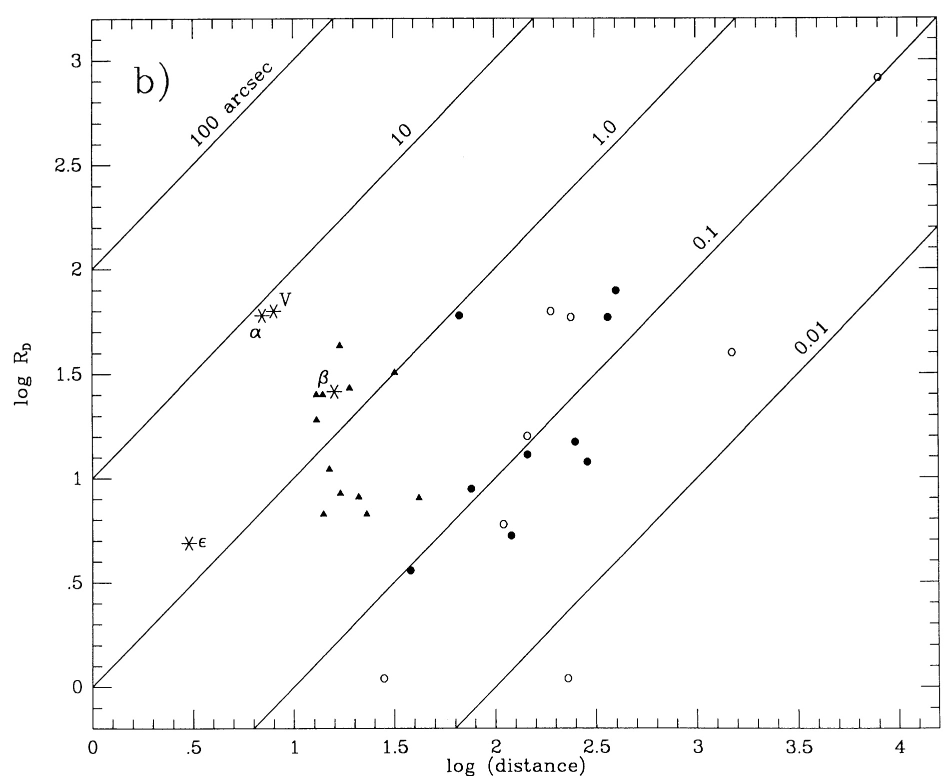


FIG. 4b–The distance to the star in parsecs is plotted against the radius of the dust shell in AU for the prototypes (*), Table I section A (●), Table I section B (○), Table II (▲), the model fitted data. The prototype stars are labeled.

TABLE III
DERIVED PROPERTIES FOR VEGA-LIKE STARS

| SAO | name | sp type | b | $M_V$ | r(pc) | $T'_*$ | $R_*/R_\odot$ | $R_D/R_\odot$ | $R_D$AU | $R_{34}$AU | CO |
|---|---|---|---|---|---|---|---|---|---|---|---|
| 234134 | $\beta$ Pic | A5V | −31 | | 16 | 8500 | 1.74 | 5701 | 26 | 19 | |
| 67174 | Vega | A0V | 19 | | 8 | 9900 | 2.51 | 13626 | 63 | 79 | N |
| 191524 | $\alpha$ PsA | A3V | −65 | | 7 | 9060 | 2.00 | 12826 | 60 | 106 | N |
| 130564 | $\epsilon$ Eri | K2V+ | −48 | | 3 | 4600 | 0.80 | 1044 | 4.9 | 9.3 | N |
| 147886 | 49 Cet | A3V | −75 | +1.5 | 67: | 9060 | 2.00 | 12826 | 60 | 68 | N |
| 112630 | HD34700 | G0 | −18 | +4.4 | (76) | 6030 | 1.05 | 1909 | 8.9 | 8.1 | N |
| 77144 | HD35187 | A2 | −6 | +1.2 | (251) | 9340 | 2.19 | 3305 | 15 | 40 | Y |
| 26804 | HD233517 | A2 | 35 | +6.5 | (38) | 4600 | 0.80 | 767 | 3.6 | 3.6 | N |
| 206462 | HD135344 | A0V | 17 | +0.7 | 398: | 9900 | 2.51 | 17025 | 79 | 117 | N |
| 226057 | HD139614 | A7V | 10 | +2.4 | 145: | 8060 | 1.58 | 2816 | 13 | 29 | |
| 183956 | HD142666 | A3 | 24 | +1.5 | (288) | 9060 | 2.00 | 2680 | 12 | 42 | N |
| 184124 | HD144432 | A9/F0V | 18 | +2.6 | 120: | 7400 | 1.35 | 1141 | 5.3 | 13 | N |
| 186777 | HD169142 | B9V | −8 | +0.3 | 363: | 11020 | 2.75 | 12626 | 59 | 108 | N |
| 179815 | HD98800 | K5V* | 34 | +7.3 | 28: | 4130 | 0.74 | 232 | 1.1 | 2.4 | N |
| 239288 | HD101584 | MIII | 6 | −4.0 | 1500: | 2500 | 40 | 8680 | 40 | 34 | |
| 256895 | HD104237 | A0pe | −16 | +0.7 | (145) | 9900 | 2.51 | 3407 | 16 | 57 | |
| 240664 | HD114855 | F5Iab | 8 | −6.2 | [8kpc:] | 6350 | 79 | 176480 | 821 | 741 | |
| 140789 | HD141569 | A0Ve | 37 | +0.7 | 191: | 9900 | 2.51 | 13629 | 63 | 47 | N |
| 226389 | HD142527 | F6III | 8 | +1.3 | 240: | 6080 | 4.37 | 12621 | 59 | 52 | |
| 183986 | HD143006 | G5e | 23 | +5.1 | (110) | 5520 | 0.93 | 1285 | 6.0 | 7.3 | N |
| 257579 | BR Oct | M5 | −25 | +11.8 | (2.5/839) | | | | | | |
| 87856 | HD188037 | A2* | −2 | +1.2 | (229) | 9340 | 2.19 | 226 | 1.1 | 105 | N |
| 21133 | $\beta$ Cas | F2IV | −3 | | 15 | 6810 | 2.34 | 2412 | 11 | | N |
| 22268 | $\delta$ Cas | A5III-IV | −2 | | 32 | 8500 | 5.50 | 6875 | 32 | | Y |
| 168373 | $\alpha$ For | F8IV* | −59 | | 14 | 6050 | 2.29 | 1450 | 6.7 | | N |
| 233457 | $\gamma$ Dor | F4III | −45 | | 17 | 6520 | 3.89 | 9162 | 43 | | |
| 5496 | HD33564 | F6V | 23 | | 19 | 6470 | 1.17 | 5796 | 27 | | N |
| 236232 | $\delta$ Vel | A1V* | −7 | | 21 | 9620 | 2.34 | 1732 | 8.1 | | |
| 99809 | $\beta$ Leo | A3V* | 71 | | 13 | 9060 | 2.00 | 4188 | 19 | | N |
| 241315 | HD121384 | G6IV-V | 7 | | (13) | 5400 | 0.92 | 5365 | 25 | | |
| 226064 | HD139664 | F5IV-V | 8 | | 17 | 6580 | 1.20 | 1804 | 8.4 | | |
| 208591 | HD155826 | F7V+G2V | 0 | | 23 | 6030 | 1.05 | 1443 | 6.7 | | Y |
| 230846 | HD207129 | G0V | −49 | | 14 | 6030 | 1.05 | 5303 | 25 | | |
| 35498 | HD221354 | K2V | −2 | | 42 | 4600 | 0.80 | 1727 | 8.0 | | Y |

Notes to table III
For r: ':' when $M_V$ with known luminosity class used,'( )' when $M_V$ assuming luminosity class V used.
SAO239288: Humphrey's distance, spectral type for the primary (MIII) alone are used.
SAO257579: if it assumed to be a dwarf the distance is 2.5pc, this is unlikely since the star is not in the Gliese catalogue. Since the star is variable it is more likely to be a giant, so the distance is 830pc.
SAO241315: no trigonometric parallax listed in the Gliese catalogue, only spectroscopic and photometric.

Space Administration (NASA), the Netherlands Agency for Aerospace Programs (NIVR), and the U.K. Science and Engineering Council (SERC). H.J.W. thanks the NASA-Ames Research Center, which provides support for *IRAS* studies through the SETI Institute under cooperative agreement NCC 2-407. The Millimeter Wave Observatory is operated by the Electrical Engineering Research Laboratory of the University of Texas at Austin with support from the National Science Foundation and McDonald Observatory. H.J.W. is grateful for hospitality from M. J. Seaton and his group at University College London and for programming support from R. de Grijp and K. Lugtenborg at the University of Leiden.

## REFERENCES

Allen, C. W. 1973, *Astrophysical Quantities* (3d ed.; London: Athlone Press).
Aumann, H. H. 1985, *Pub. A.S.P.*, **97**, 885.
Aumann, H. H., *et al.* 1984, *Ap. J. (Letters)*, **278**, L23.
Backman, D. E., and Gillett, F. C. 1987, 5th Cool Stars Workshop, Boulder, Colorado.
Backman, D. E., Gillett, F. C., and Witteborn, F. C. 1988, preprint.
Edwards, T. W. 1976, *A.J.*, **81**, 245.
Gahm, G. F., Ahlin, P., and Lindroos, K. P. 1983, *Astr. Ap. Suppl.*, **51**, 143.
Gillett, F. C. 1986, in *Light on Dark Matter*, ed. F. Israel (Dordrecht: Reidel), p. 61.
Gliese, W. 1969, *Catalogue of Nearby Stars*, Pub. Astr. Rechen-Institute, Heidelberg, No. 22.

Gradie, J., Hayashi, J. Zuckerman, B., Epps, H., and Howell, R. 1987, *Proceedings of the 18th Lunar and Planetary Sciences Conference*, (Houston, Texas: Cambridge University Press and the Lunar and Planetary Institute), p. 351.

Halprin, L., and Moon, T. T. 1983, *Ap. Space Sci.*, **91**, 43.

Heintz, W. D. 1980, *Ap. J. Suppl.*, **44**, 111.

Humphreys, R. M. 1976, *Ap. J.*, **206**, 122.

*Infrared Astronomical Satellite (IRAS) Catalogs and Atlases: The Explanatory Supplement*, 1985, ed. C. A. Beichman, G. Neugebauer, H. J. Habing, P. E. Clegg, and T. Chester (Washington, D.C.: GPO).

*Infrared Astronomical Satellite (IRAS) Catalogs and Atlases: The Point Source Catalog*, 1985 (Washington, D.C.: GPO).

Lee, T. 1970, *Ap. J.*, **162**, 217.

Odenwald, S. F. 1986, *Ap. J.*, **307**, 711.

Paresce, F., and Burrows, C. 1987, *Ap. J. (Letters)*, **319**, L23.

Sadakane, K., and Nishida, M. 1986, *Pub. A.S.P.*, **98**, 685.

Smith, B. A., and Terrile, R. J. 1984, *Science*, **226**, 1421.

Stephenson, C. B. 1986, *Ap. J.*, **300**, 779.

van de Kamp, P. 1971, *Ann. Rev. Astr. Ap.*, **9**, 103.

Walker, H. J., and Cohen, M. 1988, *A.J.*, **94**, 1801.